Incorporation of zinc into the frustule of the freshwater diatom Stephanodiscus hantzschii

Jaccard, Thomas; Ariztegui, Daniel; Wilkinson, Kevin

Chemical Geology 265 (2009) 381–386

Contents lists available at ScienceDirect

Chemical Geology

journal homepage: www.elsevier.com/locate/chemgeo

Incorporation of zinc into the frustule of the freshwater diatom *Stephanodiscus hantzschii*

Thomas Jaccard [a], Daniel Ariztegui [a,*], Kevin J. Wilkinson [b]

[a] Section of Earth & Environmental Sciences, University of Geneva, Geneva, Switzerland
[b] Department of Chemistry, University of Montreal, Montreal, Canada

ARTICLE INFO

Article history:
Received 17 November 2008
Received in revised form 22 April 2009
Accepted 24 April 2009

Editor: J. Fein

Keywords:
Diatom
Frustule
Zinc
Bioavailability
Paleolimnology

ABSTRACT

Zinc incorporation into the frustule (siliceous cell wall) of the freshwater diatom *Stephanodiscus hantzschii* was studied for Zn^{2+} concentrations ranging from 25 pmol L^{-1} to 25 nmol L^{-1}. A sigmoidal dependency was observed between Zn^{2+} concentrations in the culture medium and the concentration of Zn in the frustule. Concentrations of intracellular Zn were positively correlated with Zn in the frustule, suggesting that Zn in the frustule originated from intracellular pools. The processes leading to Zn incorporation into the cell wall were examined by determining the role(s) of Si and Mn via competition experiments. Results demonstrated that Zn competed with Mn for incorporation into the frustule. Zn/Si values for *S. hantzschii* were consistent with field data obtained from Lake Geneva (Switzerland). The study suggests that the Zn content of fossil frustules could be a valuable tool to study past levels of bioavailable Zn in freshwaters.

1. Introduction

Zn is an essential micronutrient for phytoplankton but can become inhibitory at elevated concentrations (Anderson et al., 1978; Sunda and Huntsman, 1992, 1995, 2000). Due to its widespread use in industry, anthropogenic Zn loading to freshwaters (via wastewaters or atmospheric deposition) generally dominates over natural inputs. Consequently, there is a great interest in evaluating the effects of these changes on Zn concentrations in the pelagic community. Since there is a consensus that total metal concentrations in the water are poor predictors of toxicological effects, several models have been developed to relate the chemical speciation of the metals to their bioavailability (for a review, see Slaveykova and Wilkinson, 2005).

Nonetheless, there is still a lack of reliable tools to evaluate the influence of Zn – and other trace metals – on phytoplankton growth and community composition during past environmental and climatic perturbations. One major obstacle is the difficulty in relating sediment analyses with past concentrations of bioavailable or intracellular metals. Ellwood and Hunter (2000a) have investigated the incorporation of Zn and Fe into the frustule (siliceous cell wall) of the marine diatom, *Thalassiosira pseudonana*. Zn levels in the cell wall generally increased over a wide range of free Zn^{2+} concentrations in culture media, leading the authors to suggest that Zn content in fossil frustules could be used to track past changes in oceanic concentrations of free Zn^{2+}. This novel proxy was subsequently applied to Southern Ocean samples spanning the last interglacial-glacial transition (Ellwood and Hunter, 2000b) where the authors did not find any evidence to support the "zinc hypothesis" (i.e., Zn stimulation of export production during the ice ages; Morel et al., 1994). The goal of this study was to investigate further whether Zn concentrations of the frustules can be employed as a paleolimnological indicator of bioavailable Zn. Since it is essential to understand the uptake process in order to correctly interpret fossil samples, the influence of Zn^{2+} concentrations and the role of Mn^{2+} and Si on Zn incorporation by the frustule were systematically evaluated for the common freshwater diatom, *Stephanodiscus hantzschii*.

2. Methodology

2.1. Zn uptake experiments

Zn uptake by *Stephanodiscus hantzschii* (UTCC 267) was evaluated in a modified CHU-10 medium (Nichols, 1973). Free Zn^{2+} ion concentrations were systematically varied by concomitant addition of Zn and EDTA (ethylene diamine tetraacetic acid) over a Zn^{2+} concentration range ($10^{-10.6}$–$10^{-7.6}$ mol L^{-1}) that was characteristic of natural freshwaters (Xue and Sigg, 1994; Xue et al., 1995). Calculated free ion concentrations (MINTEQA2; Allison et al., 1991) are reported in Table 1. All experiments were carried out at pH = 6.4 at 20 °C in acid-cleaned polycarbonate flasks with 100 rpm rotary

* Corresponding author. Section of Earth & Environmental Sciences, University of Geneva, Rue des Maraichers 13, CH-1205 Geneva, Switzerland. Tel.: +41 22 379 66 18; fax: +41 22 379 32 10.
E-mail address: daniel.ariztegui@unige.ch (D. Ariztegui).

0009-2541/$ – see front matter © 2009 Elsevier B.V. All rights reserved.
doi:10.1016/j.chemgeo.2009.04.016

Table 1
Composition of the experimental medium used for Zn uptake experiments.

Macro-nutrients	Total concentrations
NO_3^-	488 μmol L^{-1}
PO_4^{3-}	57 μmol L^{-1}
$Si(OH)_4$	207 μmol L^{-1}
Metals	log [M^{n+}]
Na^+	−3.08
Mg^{2+}	−4.00
K^+	−3.94
Ca^{2+}	−3.62
Mn^{2+}	−6.18
Fe^{3+}	−18.99
Co^{2+}	−10.44
Cu^{2+}	−12.56
Zn^{2+}	Varied between −10.62 and −7.61
Chelator	Total concentration
EDTA	Varied between 12.4 and 89.3 μmol L^{-1}

shaking. Lighting was provided on a 12:12 h light:dark cycle using 50 μmol photons m^{-2} s^{-1} of white fluorescent lighting. At mid-exponential growth, cells were transferred from a modified CHU-10 culture medium with a pZn of 9.62 to 50 mL of experimental medium containing the desired Zn^{2+} concentration and a cell density of ca. 2×10^4 cells mL^{-1}. After again attaining mid exponential growth phase, the cells were then transferred to 300 mL of experimental medium. Experiments were performed under laminar flow and other precautions in order to avoid both biological and chemical contamination. Cell numbers were measured daily using an electronic particle counter (Coulter Multisizer 2). The specific growth rate was calculated from the linear regression of (ln) cell number as a function of time. *S. hantzschii* was grown for 6 or more generations and harvested at the end of the exponential growth phase. A 50 mL aliquot was collected from the final 300 mL of cell culture for analyses of intracellular metal content. In that case, cells were centrifuged and washed with 10 mL of a metal-free medium containing 10^{-3} mol L^{-1} EDTA (Hassler et al., 2004). Intracellular metal contents were determined by ICP-MS (inductively coupled plasma mass spectrometer; Hewlett Packard, 4500; detection limits for Zn and Mn of 0.1 ppb) following digestion of the pellet for 1 h in concentrated ultrapure HNO_3 at 80 °C. The remaining 250 mL of cell culture were filtered over a 3 μm nitrocellulose membrane that was subsequently digested for 1 h in concentrated HNO_3 at 80 °C. The residual silica was then washed 4 times with MilliQ water and dissolved in a 0.1 mol L^{-1}/0.1 mol L^{-1} HCl/HF solution for 4 h at 80 °C. We preferred hot HCl/HF rather than an NaOH dissolution (Paasche, 1973) since with the latter, silica polymerization was occasionally observed when samples were cooled to room temperature. Nonetheless, the possible loss of Si from solution due to the formation of volatile SiF_4 was investigated. Under the conditions used in this experiment, Si recovery was, within error, 100%, attesting to the reliability of the digestion process. After dissolution, samples were centrifuged and visually inspected to ensure silica dissolution. In the solution containing the dissolved silica, Zn and Mn concentrations were measured by ICP-MS while Si was determined in diluted (100 times) samples using a molybdate-blue spectrophotometric method at 820 nm (Merck, Spectroquant 14794 with a Perkin Elmer Lambda 35 spectrophotometer). Blank HNO_3 and HF/HCl digests were systematically verified for metal contamination. For a limited number of samples, intracellular and frustule metal concentrations could not be measured on the same 300 mL aliquot of sample. In those cases, additional experiments were prepared under identical conditions in order to analyze intracellular metal content.

Table 2
Zn^{2+}, Mn^{2+} and $Si(OH)_4$ concentrations of the experimental media used for the experiments in which the role of Mn^{2+} and Si on Zn incorporation were evaluated.

Experiment	log[Zn^{2+}]	log[Mn^{2+}]	[$Si(OH)_4$] (mmol L^{-1})
Zn uptake experiment (control)	−9.23	−6.18	0.21
	−8.93	−6.18	0.21
Role of Mn^{2+} on Zn incorporation	−9.23	−5.21	0.21
	−8.93	−5.20	0.21
Role of Si on Zn incorporation	−9.23	−6.18	2.10
	−8.93	−6.18	2.10

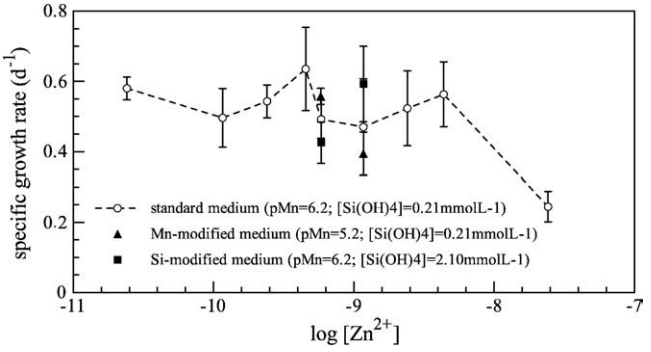

Fig. 1. Specific growth rate (d^{-1}) of *Stephanodiscus hantzschii* as a function of log[Zn^{2+}] for Zn uptake experiments (open circles and dashed line, pMn = 6.2, [$Si(OH)_4$] = 0.21 mmol L^{-1}) or for experiments examining the role of a modification in Mn^{2+} (filled triangles, pMn = 5.2, [$Si(OH)_4$] = 0.21 mmol L^{-1}) or $Si(OH)_4$ concentrations (filled squares, pMn = 6.2, [$Si(OH)_4$] = 2.10 mmol L^{-1}). Error bars indicate the 95% confidence interval (CI). No significant differences ($p>0.05$, *t*-test) were found between specific growth rates for Zn uptake experiment and those obtained when [$Si(OH)_4$] or [Mn^{2+}] were varied.

2.2. Role of Mn and Si on Zn incorporation

In experiments designed to determine the role of Si and Mn on Zn incorporation, $Si(OH)_4$ and Mn^{2+} concentrations were 10 times higher than were generally used in the experimental medium (Table 2). These competition experiments were performed at pZn levels of 8.93 and 9.23. In spite of $Si(OH)_4$ concentrations approaching saturation in the more concentrated media, no silica precipitation was observed. Metal concentrations were systematically verified in the experimental media using ICP-MS to ensure that the observed variations were due to systematic changes to the Si and Mn concentrations rather than contamination.

3. Results

3.1. Specific growth rate

Maximal growth rates were observed over the entire range of examined Zn^{2+} concentrations, except at a pZn of 7.61, where the growth decreased (Fig. 1). No significant effect ($p>0.05$, *t*-test) on the specific growth rate was observed for a 10 fold increase of [Mn^{2+}] (pZn = 9.23, $p=0.054$, $df=8$, *t*-test; pZn = 8.93, $p=0.320$, $df=7$, *t*-test) or [$Si(OH)_4$] (pZn = 9.23, $p=0.139$, $df=7$, *t*-test; pZn = 8.93, $p=0.217$, $df=6$, *t*-test).

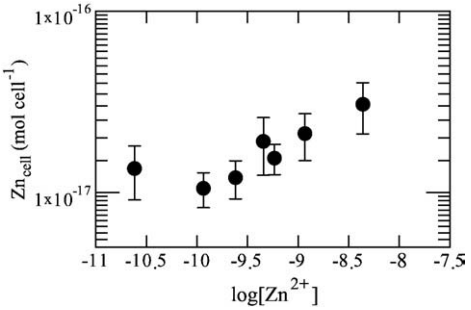

Fig. 2. Intracellular zinc, Zn_{cell}, as a function of log[Zn^{2+}] for *Stephanodiscus hantzschii*. Error bars indicate 95% CI.

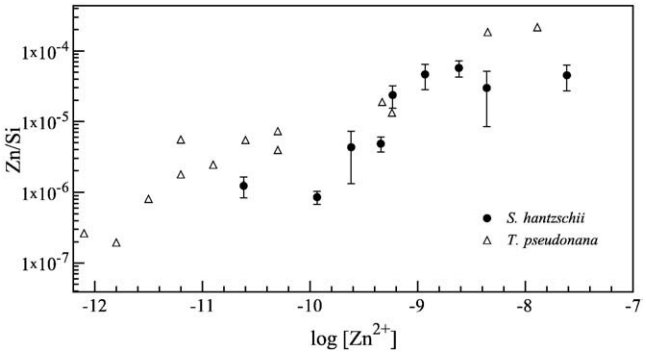

Fig. 3. Frustule Zn/Si molar ratio as a function of $\log[Zn^{2+}]$ for *Stephanodiscus hantzschii* (filled circles). Error bars indicate 95% CI. The results of Ellwood and Hunter (2000a) for *Thalassiosira pseudonana* are reported by the open triangles.

3.2. Zn uptake

For Zn uptake experiments, intracellular Zn concentrations, Zn_{cell}, generally increased as a function of the Zn^{2+} concentration in the medium (Fig. 2). Nonetheless, Zn_{cell} had only a weak dependence on Zn^{2+} concentrations in the medium: a nearly 200 fold increase in free Zn led to only a four-fold increase of intracellular Zn. Intracellular Zn determinations for pZn values of 8.62 and 7.61 were discarded because blank samples were contaminated by Zn. A sigmoidal relationship was observed between the molar Zn/Si ratio of the frustule when plotted as a function of the Zn^{2+} concentration in the medium. A maximal slope was observed for pZn values between 9.9 and 8.9 (Fig. 3). Similar Zn/Si data, obtained for the marine diatom *Thalassiosira pseudonana* (Ellwood and Hunter, 2000a), are reported for comparison. To assess the dependency of the Zn in the frustule on the intracellular Zn, these parameters were reported in a log–log plot (Fig. 4). Only data from experiments for which Zn concentrations were measured on identical samples for both the frustule and the cell have been reported. Zn contents of the frustule were not normalized to the Si content, but rather provided on a per cell basis. Nonetheless, the cellular Si content ($(2.0\pm0.2)\times10^{-13}$ mol Si cell^{-1}) did not vary over the course of the experiment and was consistent with the values found by Twining et al. (2003) for the same *S. hantzschii* clone. A strong positive correlation (Spearman correlation coefficient, $r_s=0.87$) was observed between the Zn associated with the cell wall, Zn_{frust}, and the intracellular Zn, Zn_{cell}.

3.3. Role of Mn and Si on Zn incorporation

For the Zn uptake experiments, neither the intracellular Mn nor the normalized molar Mn/Si cell wall ratio varied greatly over the range of

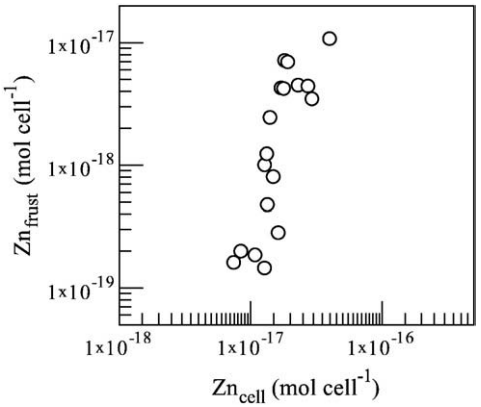

Fig. 4. Zn frustule content, Zn_{frust}, as a function of the intracellular Zn concentration, Zn_{cell}, for *Stephanodiscus hantzschii*. A Spearman correlation coefficient of $r_s=0.87$ was obtained for the association of these two variables.

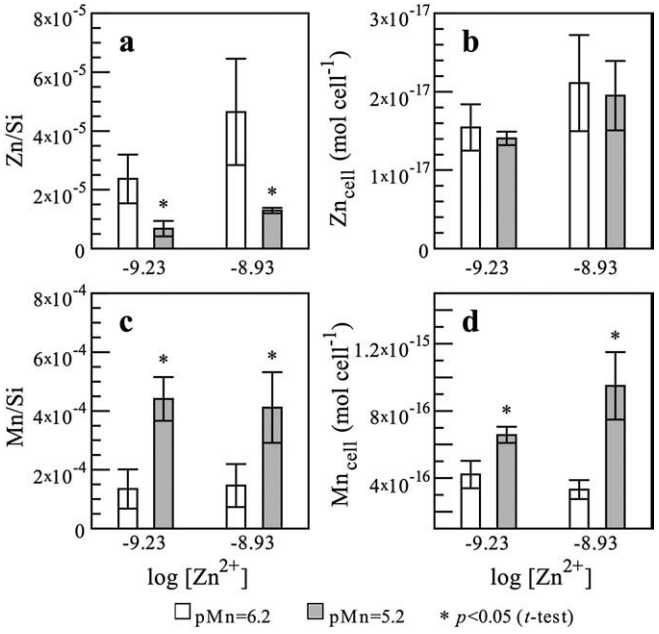

Fig. 5. Values of (a) frustule Zn/Si molar ratio, (b) intracellular Zn, Zn_{cell}, (c) frustule Mn/Si molar ratio and (d) intracellular Mn, Mn_{cell} of *Stephanodiscus hantzschii* for two concentrations of Zn^{2+} (*x*-axis) and two Mn^{2+} concentrations (white bars or control: pMn = 6.2; grey bars: pMn = 5.2). The stars denote significant differences ($p<0.05$, *t*-test) with respect to the control.

studied $[Zn^{2+}]$ (data not shown). Nonetheless, the addition of Mn^{2+} significantly ($p<0.05$, *t*-test) decreased the Zn/Si ratio (Fig. 5a; pZn = 9.23, $p=0.026$, $df=6$, *t*-test; pZn = 8.93, $p=0.011$, $df=8$, *t*-test) even though intracellular Zn concentrations were not affected (Fig. 5b; pZn = 9.23, $p=0.479$, $df=5$, *t*-test; pZn = 8.93, $p=0.699$, $df=4$, *t*-test). As expected, higher $[Mn^{2+}]$ in the medium also led to higher values of Mn in the frustule (Fig. 5c; pZn = 9.23, $p=0.001$, $df=6$, *t*-test; pZn = 8.93, $p=0.005$, $df=8$, *t*-test) and in the cell (Fig. 5d; pZn = 9.23, $p=0.007$, $df=5$, *t*-test; pZn = 8.93, $p=0.004$, $df=4$, *t*-test). Increased

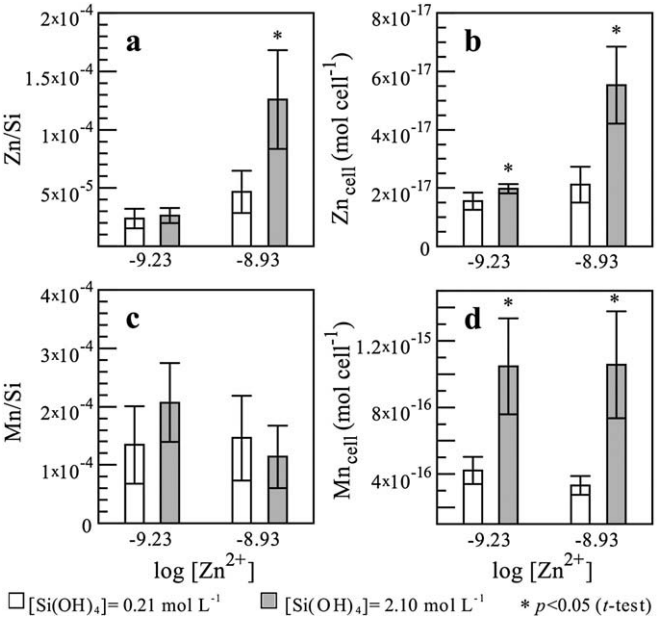

Fig. 6. Values of (a) frustule Zn/Si molar ratio, (b) intracellular Zn, Zn_{cell}, (c) frustule Mn/Si molar ratio and (d) intracellular Mn, Mn_{cell} of *Stephanodiscus hantzschii* for two concentrations of Zn^{2+} (*x*-axis) and two $Si(OH)_4$ concentrations (white bars or control: $[Si(OH)_4]=0.21$ mmol L^{-1}; grey bars: $[Si(OH)_4]=2.10$ mmol L^{-1}). The stars denote significant differences ($p<0.05$, *t*-test) with respect to the control.

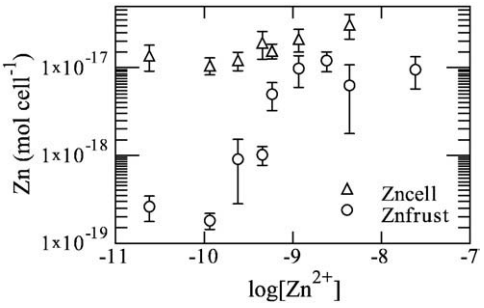

Fig. 7. Intracellular zinc, Zn_{cell}, and zinc in the frustule, Zn_{frust}, as a function of $\log[Zn^{2+}]$ for *Stephanodiscus hantzschii*. Error bars indicate 95% CI.

concentrations of $Si(OH)_4$ in the medium resulted in an increased accumulation of intracellular Zn (Fig. 6b; pZn = 9.23, $p = 0.047$, $df = 6$, *t*-test; pZn = 8.93, $p = 0.011$, $df = 7$, *t*-test), with a greater effect observed at pZn = 8.93. A significant effect on the concentration in the frustule was only observed for Zn at pZn = 8.93 (Fig. 6a; pZn = 9.23, $p = 0.662$, $df = 7$, *t*-test; pZn = 8.93, $p = 0.003$, $df = 9$, *t*-test), in which case a higher Zn/Si value was perceived. A higher concentration of $Si(OH)_4$ in the medium lead to higher values of intracellular Mn (Fig. 6d; pZn = 9.23, $p = 0.006$, $df = 6$, *t*-test; pZn = 8.93, $p = 0.006$, $df = 7$, *t*-test), even though no significant effect on the Mn/Si ratio in the frustule was noticed (Fig. 6c; pZn = 9.23, $p = 0.185$, $df = 7$, *t*-test; pZn = 8.93, $p = 0.568$, $df = 9$, *t*-test).

4. Discussion

4.1. Zn uptake experiment

From the weak slope in Fig. 2, it was clear that intracellular Zn concentrations, Zn_{cell}, were highly regulated over the studied range of Zn^{2+} concentrations for this diatom. Values of cellular Zn were consistent with those found by Twining et al. (2003) for the same *S. hantzschii* clone grown in the WCL-1 medium (Guillard, 1975). In addition, a similar trend was observed for Zn uptake by phytoplankton in seawater where Sunda and Huntsman (1992) obtained a sigmoidal dependency between intracellular Zn and Zn^{2+} concentrations in seawater. In that study, which examined several species of diatoms and a coccolithophore, minimal slopes were consistently observed in the pZn range of 10.5–9.5 while larger slopes were determined above and below this range. The shape of the curves has been interpreted to indicate that there were at least two separate uptake systems for Zn with widely different affinity constants. In that case, the minimal slopes at intermediate $[Zn^{2+}]$ were attributed to a negative feedback regulation of the high affinity Zn uptake system whereas the increased slope at higher Zn concentrations corresponded to Zn uptake by the low-affinity site. In this paper, no evidence for a second uptake system was obtained, albeit the examined concentration range was smaller than that studied by Sunda and Huntsman. The shape of the Zn/Si vs. $[Zn^{2+}]$ curve for *S. hantzschii* (Fig. 3) was very similar to that obtained for the marine diatom, *T. pseudonana* (Ellwood and Hunter, 2000a), even though slightly lower Zn/Si ratios were observed here. The similarity in the shape of the two Zn/Si datasets suggests a common mechanism of Zn incorporation into the frustule of the two diatom species. The discrepancy between the absolute values of the Zn/Si ratios for the two diatoms can be explained by a number of factors including the different media used in the two studies. For example, the medium employed here contained nearly 200 times more Mn^{2+} than the experimental medium used to grow *T. pseudonana*. Recall that in our Mn variation experiments, higher concentrations of Mn^{2+} in the medium significantly lowered the Zn/Si ratio (Fig. 5a). Other factors such as a species-specific variability cannot be excluded. The strong positive correlation between Zn in the frustule and that in the cell (Fig. 4) is consistent with a mechanism in which the internal intracellular Zn pools are used to supply Zn to the cell wall (Ellwood and Hunter, 2000a). A plot of Zn_{frust} and Zn_{cell} against $[Zn^{2+}]$ (Fig. 7) demonstrated that Zn_{frust} represented between 1 and 27% of the cell's Zn reserves (i.e. $Zn_{frust} + Zn_{cell}$). The leveling off in the Zn/Si curve for Zn^{2+} concentrations exceeding ca. 10^{-9} mol L^{-1}, which did not appear to occur for the intracellular Zn data (intracellular concentration for a pZn of 8.36 is significantly higher than for a pZn of 9.23; $p = 0.019$, $df = 5$, *t*-test) provides some evidence for a saturable system of Zn incorporation into the frustule.

4.2. Role of Mn on Zn incorporation

As discussed earlier, it is thought that at least two transport systems control Zn entry into the cell. In addition to these two primary Zn transporters, at low Mn^{2+}concentrations, Zn is able to use a Mn transporter in the green alga, *Chlamydomonas* sp. (Sunda and Huntsman, 1998). For the range of Zn concentrations examined in this study, Zn was likely taken up by the low-affinity system since intracellular Zn did not change significantly with variable $[Mn^{2+}]$, suggesting that either this pathway is not used in *S. hantzschii* or that only relatively small concentrations of Zn entered the cell by the Mn uptake pathway. Indeed, while higher concentrations of Mn^{2+} did not affect intracellular Zn levels, they increased both intracellular Mn and Mn/Si while decreasing Zn/Si. These variations suggested that Mn and Zn competed for incorporation by the frustule.

4.3. Nature of Zn incorporation

The mechanism of Zn incorporation into the diatom cell walls is not clear. In the literature, arguments have been advanced for both passive and active metal incorporation processes. The first mechanism implies that the metals are passively added to the frustule structure while in the active process metals are involved in the formation of the frustule. In the passive incorporation process, it is likely that several different metals would be present in the frustule (Ellwood and Hunter, 2000a). For example, in addition to Mn (detected in this study), Al and Ge have been found in diatom frustules (Azam et al., 1973; Gehlen et al., 2002). Investigation of the atomic structure of the biogenic silica revealed a structural association between Al and Si (Gehlen et al., 2002), which was interpreted as an incorporation of Al during the biosynthesis of the frustule (Gehlen et al., 2002). Since Al, Ge and Si have the same coordination numbers with oxygen and similar atomic diameters, they can easily substitute for Si in the frustule structure. In contrast to Ge and Al, the atomic radius of Zn (tetrahedral geometry) is almost twice that of Si and thus its substitution is less likely. Nevertheless, Lal et al. (2006) have suggested that the substantial interstitial spaces in the polymerizing silica structure could easily accommodate larger metal ions.

Arguments that support an active role of Zn frustule formation include long-term incubation studies showing that silicic acid ($Si(OH)_4$) uptake by *T. pseudonana* was reduced for Zn deficient cultures and by Cu toxicity (Rueter and Morel, 1981). These same authors observed that Zn-limited *T. weissflogii* morphologically resembled Cu-inhibited or Si-starved *T. pseudonana*. Fisher et al. (1981) could not distinguish between Cu-treated cells and Si-limited cells of the diatom *Asterionella japonica*. These results led to the hypothesis that silicic acid uptake was mediated by a Zn-dependent system that could be inactivated by copper. Nonetheless, a recent study showed that Zn concentrations had no influence on short-term Si uptake kinetics (Thamatrakoln and Hildebrand, 2007). Such a result suggested that previous long-term studies were reflecting the influence of Zn on Si cell wall incorporation kinetics rather than on biological uptake. This alternative explanation is supported by a recent investigation of the effect of Zn deficiency on silica production (De La Rocha et al., 2000) and is consistent with the competition between Zn and Mn for entry into the cell wall that was observed in this study. If Zn plays an active role in frustule formation (for

example, as an enzyme co-factor), one would indeed expect Mn to be able to substitute for Zn. Some proteins or peptides have been shown to be tightly associated with the frustules with their release only occurring following the complete dissolution of the silica. It is possible that Zn incorporation into the frustule might be via one of these HF- or NH_4F-extractable organic macromolecules. These compounds include some of the major components involved in silica polymerization: silaffins (Kroger et al., 2001, 2002; Frigeri et al., 2006), long-chain polyamines (Kroger et al., 2000; Ingalls et al., 2004), pleuralins (Kroger et al., 1997; Kroger and Wetherbee, 2000) and several other unidentified molecules (Swift and Wheeler, 1992; Frigeri et al., 2006). Whereas the association of pleuralins with the frustule is due to their high affinity for silica, long chain polyamines and silaffins are thought to be fully encapsulated in the silica spheres (Vrieling et al., 2002).

Although Zn incorporation into the cell wall of *S. hantzschii* can be explained by a passive uptake, the tight relationship between Zn_{cell} and Zn_{frust}, the "saturable" nature of the Zn deposition process and the observed competition between Mn and Zn incorporation into the frustule suggests that Zn incorporation was most probably active. Zn containing organic macromolecules could possibly mediate this process.

4.4. Role of Si on Zn incorporation

The addition of silicic acid to the medium increased the intracellular content of both the Zn and Mn (Fig. 6b, d). The reason for the increased accumulation under the higher silicic acid regime is not clear. In the frustule, a significant difference was only obtained for Zn at pZn levels of 8.93 (Fig. 6a, c), in which case higher Zn/Si ratios were measured. Because the addition of silicic acid had no significant effect on the Si content of the frustules (pZn = 9.23, $p = 0.724$, $df = 5$, t-test; pZn = 8.93, $p = 0.844$, $df = 5$, t-test; data not shown), these changes must reflect higher Zn uptake to the cell wall rather than modifications to Si deposition. Consistent with our previously discussed hypothesis of Zn incorporation, the observed decoupling between Mn concentrations in the cell and the frustule (higher intracellular concentrations but no change in the frustule content) likely reflects a competition of Zn and Mn for cell wall incorporation. Indeed, high intracellular Zn concentrations prevented Mn from being incorporated into the cell wall. The Zn/Si ratio found for the experiment performed at a pZn of 8.93 (Fig. 6a) was the highest measured in this study and indeed higher than the apparent maximum found during the Zn uptake experiment (Fig. 3), suggesting that an additional effect was associated with the higher silicic acid concentrations in the medium. For example, Si could be postulated to regulate the production of the hypothetical Zn-dependent macromolecule responsible for metal incorporation into the frustule, which would consequently influence both Zn/Si and Mn/Si ratios in the cell wall.

4.5. Environmental relevance

Recently, we measured the Zn/Si ratio of fossil frustules isolated from Lake Geneva (Switzerland) sediments (Jaccard et al., 2009). The values ranged from 0.6 to 9.8 μmol mol^{-1}, consistent with the values obtained here for *S. hantzschii*. Based upon Zn/Si data from Fig. 3, it is therefore possible to estimate Zn^{2+} concentrations in surface waters. Indeed, these reconstructions are consistent with modern field data, strongly suggesting that the proxy may become a valuable tool to assess past changes in bioavailable Zn concentrations in freshwater systems (Jaccard et al., 2009). Due to the sigmoidal shape of the uptake curve (Fig. 3), this indicator is particularly sensitive for variations of Zn^{2+} concentrations in the 10^{-10}–10^{-9} M range.

5. Conclusion

Our investigations showed that Zn is incorporated into the frustule of the freshwater diatom *Stephanodiscus hantzschii*. The sigmoidal relationship between Zn^{2+} concentrations in the growth medium and the Zn incorporated into the cell wall, Zn/Si, is consistent with previous results on *Thalassiosira pseudonana*, suggesting a common mechanism of Zn incorporation into the frustule of these two diatoms. In addition, the strong dependency of the Zn frustule content on the intracellular concentration of Zn indicates that the Zn that was incorporated into the cell wall was from an intracellular source. Experiments examining the effects of Mn and Si on Zn uptake to the frustule were consistent with a mechanism in which intracellular Zn and Mn would compete for cell wall incorporation. Measurements of the Zn/Si ratio of fossil frustules from sediments are likely to be a useful proxy for bioavailable Zn concentrations of surface waters. Nonetheless, further field and laboratory data are still required to obtain a better biological and chemical understanding of the processes that control Zn incorporation into the frustules and potential diagenetic overprints. This approach can therefore provide a suitable tool to study past Zn-phytoplankton interactions.

Acknowledgements

We thank I. Worms for helpful discussions and suggestions, S. L. Jaccard and D. Semeniuk for their comments on previous versions of the manuscript. This work was founded by the Swiss National Science Foundation projects TRADIA I and II (200021-107475 and 200020-116350, respectively).

References

Allison, J.D., Brown, D.S., Novo-Gradac, K.J., 1991. MINTEQA2/ PRODEFA2, a geochemical assessment model for environmental systems: Version 3.0 Users manual. US Environmental Protection Agency, Athens, GA. EPA/600/3-91/021.

Anderson, M.A., Morel, F.M.M., Guillard, R.R.L., 1978. Growth limitation of a coastal diatom by low zinc ion activity. Nature 276, 70–71.

Azam, F., Hemmingsen, B.B., Volcani, B.E., 1973. Germanium incorporation into the silica of diatom cell walls. Arch. Microbiol. 92 (1), 11–20.

De La Rocha, C.L., Hutchins, D.A., Brzezinski, M.A., Zhang, Y., 2000. Effects of iron and zinc deficiency on elemental composition and silica production by diatoms. Mar. Ecol. Prog. Ser. 195, 71–79.

Ellwood, M.J., Hunter, K.A., 2000a. The incorporation of zinc and iron into the frustule of the marine diatom *Thalassiosira pseudonana*. Limnol. Oceanogr. 45 (7), 1517–1524.

Ellwood, M.J., Hunter, K.A., 2000b. Variations in the Zn/Si record over the last interglacial glacial transition. Paleoceanography 15 (5), 506–514.

Fisher, N.S., Jones, G.J., Nelson, D.M., 1981. Effects of copper and zinc on growth, morphology, and metabolism of *Asterionella japonica (Cleve)*. J. Exp. Mar. Biol. Ecol. 51, 37–56.

Frigeri, L.G., Radabaugh, T.R., Haynes, P.A., Hildebrand, M., 2006. Identification of proteins from a cell wall fraction of the diatom *Thalassiosira pseudonana*. Mol. Cell. Proteomics 5 (1), 182–193.

Gehlen, M., Beck, L., Calas, G., Flank, A.-M., Van Bennekom, A.J., Van Beusekom, J.E.E., 2002. Unraveling the atomic structure of biogenic silica: evidence of the structural association of Al and Si in diatom frustules. Geochim. Cosmochim. Acta 66 (9), 1601–1609.

Guillard, R.R.L., 1975. In: Smith, W.L., Chanley, M.H. (Eds.), Culture of marine invertebrate animals. InPlenum.

Hassler, C.S., Slaveykova, V.I., Wilkinson, K.J., 2004. Discriminating between intra- and extracellular metals using chemical extractions. Limnol. Oceanogr. Meth. 2, 237–247.

Ingalls, A.E., Anderson, R.F., Pearson, A., 2004. Radiocarbon dating of diatom-bound organic compounds. Mar. Chem. 92 (1–4), 91–105.

Jaccard, T., Ariztegui, D., Wilkinson, K.J., 2009. Assessing past changes in bioavailable zinc from a terrestrial $(Zn/Si)_{opal}$ record. Chem. Geol. 258, 362–367. doi:10.1016/j.chemgeo.2008.1010.1037.

Kroger, N., Wetherbee, R., 2000. Pleuralins are involved in theca differentiation in the diatom *Cylindrotheca fusiformis*. Protist 151 (3), 263–273.

Kroger, N., Lehmann, G., Rachel, R., Sumper, M., 1997. Characterization of a 200-kDa diatom protein that is specifically associated with a silica-based substructure of the cell wall. Eur. J. Biochem. 250 (1), 99–105.

Kroger, N., Deutzmann, R., Bergsdorf, C., Sumper, M., 2000. Species-specific polyamines from diatoms control silica morphology. Proc. Natl. Acad. Sci. USA 97 (26), 14133–14138.

Kroger, N., Deutzmann, R., Sumper, M., 2001. Silica-precipitating peptides from diatoms: the chemical structure of silaffin-1A from *Cylindrotheca fusiformis*. J. Biol. Chem. 276 (28), 26066–26070.

Kroger, N., Lorenz, S., Brunner, E., Sumper, M., 2002. Self-assembly of highly phosphorylated silaffins and their function in biosilica morphogenesis. Science 298 (5593), 584–586.

Lal, D., Charles, C., Vacher, L., Goswami, J.N., Jull, A.J.T., McHargue, L., Finkel, R.C., 2006. Paleo-ocean chemistry records in marine opal: Implications for fluxes of trace

elements, cosmogenic nuclides (^{10}Be and ^{26}Al), and biological productivity. Geochim. Cosmochim. Acta 70, 3275–3289.
Morel, F.M.M., Reinfelder, J.R., Roberts, S.B., Chamberlain, C.P., Lee, J.G., Yee, D., 1994. Zinc and carbon co-limitation of marine phytoplankton. Nature 369, 740–742.
Nichols, H.W., 1973. Growth media — freshwater. In: Stein, J.R. (Ed.), Handbook of Phycological Methods-Culture Methods and Growth Measurements. Cambridge University Press.
Paasche, E., 1973. Silicon and the ecology of marine plankton diatoms. I. *Thalassiosira pseudonana* (*Cyclotella nana*) grown in a chemostat with silicate as limiting nutrient. Mar. Biol. 19 (2), 117–126.
Rueter, J.G.J., Morel, F.M.M., 1981. The interaction between zinc deficiency and copper toxicity as it affects the silicic acid uptake mechanisms in *Thalssiosira pseudonana*. Limnol. Oceanogr. 26 (1), 67–73.
Slaveykova, V.I., Wilkinson, K.J., 2005. Predicting the bioavailability of metals and metal complexes: critical review of the biotic ligand model. Environ. Chem. 2, 9–24.
Sunda, W.G., Huntsman, S.A., 1992. Feedback interactions between zinc and phytoplankton in seawater. Limnol. Oceanogr. 37 (1), 25–40.
Sunda, W.G., Huntsman, S.A., 1995. Cobalt and zinc interreplacement in marine phytoplankton: biological and geochemical implications. Limnol. Oceanogr. 40 (8), 1404–1417.
Sunda, W.G., Huntsman, S.A., 1998. Interactions among Cu^{2+}, Zn^{2+}, and Mn^{2+} in controlling cellular Mn, Zn, and growth rate in the coastal alga *Chlamydomonas*. Limnol. Oceanogr. 43 (6), 1055–1064.
Sunda, W.G., Huntsman, S.A., 2000. Effect of Zn, Mn, and Fe on Cd accumulation in phytoplankton: implications for oceanic Cd cycling. Limnol. Oceanogr. 45, 1501–1516.
Swift, D.M., Wheeler, A.P., 1992. Evidence of an organic matrix from diatom biosilica. J. Phycol. 28, 202–209.
Thamatrakoln, K., Hildebrand, M., 2007. Silicon uptake in diatoms revisited: a model for saturable and nonsaturable uptake kinetics and the role of silicon transporters. Plant Physiol. 107.107094.
Twining, B.S., Baines, S.B., Fisher, N.S., Maser, J., Vogt, S., Jacobsen, C., Tovar-Sanchez, A., SaÕudo-Wilhelmy, S.A., 2003. Quantifying trace elements in individual aquatic protist cells with a synchrotron X-ray fluorescence microprobe. Anal. Chem. 75, 3806–3816.
Vrieling, E.G., Beelen, T.P.M., van Santen, R.A., Gieskes, W.W.C., 2002. Mesophases of (bio)polymer-silica particles inspire a model for silica biomineralization in diatoms. Angew. Chem. Int. Ed. 41 (9), 1543–1546.
Xue, H.B., Sigg, L., 1994. Zinc speciation in lake waters and its determination by ligand exchange with EDTA and differential pulse anodic stripping voltammetry. Anal. Chim. Acta 284 (3), 505–515.
Xue, H.B., Kistler, D., Sigg, L., 1995. Competition of copper and zinc for strong ligands in a eutrophic lake. Limnol. Oceanogr. 40 (6), 1142–1152.